

The Dark Ages: Searching for the Epoch of First Light

A Meiksin

*Institute for Astronomy, University of Edinburgh, Royal Observatory,
Edinburgh EH9 3HJ*

Abstract. Prior to the epoch of full reionization, the intergalactic medium and gravitationally collapsed systems will be detectable in 21-cm radiation. Physical mechanisms that would produce a 21-cm signature are discussed. These include Ly α coupling of the hydrogen spin temperature to the kinetic temperature of the gas resulting from the radiation by an early generation of stars, preheating by soft x-rays from collapsing dark matter halos, and preheating by ambient Ly α photons. A patchwork of either 21-cm emission, or absorption against the Cosmic Microwave Background, will result. Large radio telescopes like the Giant Metre Wavelength Telescope (GMRT) or a Square Kilometre Array Radio Telescope (SKA) offer the prospect of measuring this signature, and so detecting the transitional epoch from a dark universe to one with light.

Invited review talk at the International SKA Science Meeting, Calgary, 19–22 July 1998. Included in the SKA Radio Telescope Science Case, ed. R. Braun.

1. Introduction

The development of structure in the Universe was well advanced at early times. Quasars have been detected nearly to a redshift of $z = 5$, and the most distant galaxies to even greater redshifts (Dey *et al.* 1998). The spectra of high redshift QSOs have additionally shown that the Intergalactic Medium (IGM) itself had undergone an extensive development of nonlinear structures at early times as well, as revealed by the Ly α forest. Still unknown, however, is the nature of energetic processes at these early times. While numerical simulations have shown that the IGM is expected to fragment into structures at early times in Cold Dark Matter (CDM) dominated cosmologies (Zhang *et al.* 1998), and even into early galaxies (Governato *et al.* 1997), the simulations are much less able to predict the efficiency with which gravitationally collapsed objects will emit radiation. Although QSO sources may account for the photoionizing UV background at high redshifts (Meiksin & Madau 1993; Haardt & Madau 1997), it is less clear that they were responsible for the original reionization of the IGM. Similarly, although $z > 5$ galaxies have been detected, the epoch during which the first generation of stars formed is still poorly constrained (Madau *et al.* 1998; Hughes *et al.* 1998). Although IR observations will permit even higher redshift galaxies and QSOs to be observed, detections become increasingly difficult because of the

diminution in surface brightness due to cosmological expansion. This difficulty calls for alternative means to be found for discovering the nature and period of the first major generation of energy-producing sources, the epoch of First Light.

I discuss here possible ways in which a Square Kilometre Array (SKA) radio telescope could reveal the first epochs of energy generation. Because so little is known about the distribution and nature of such sources, the emphasis will be on the physical mechanisms related to their detection. The means by which the sources are revealed is through their impact on the surrounding neutral IGM and the resulting emission or absorption of 21-cm radiation. In the next section, I review the Wouthuysen-Field mechanism for the excitation of 21-cm emission through the scattering of Ly α photons, and the heating of the neutral IGM by resonant scattering of the Ly α photons and soft x-ray heating from early collapsed objects. In §III, a few scenarios are presented for the possible effects of early generations of radiation sources on the IGM and their detection.

2. 21-cm Emission and Absorption Mechanisms

2.1. The Spin Temperature

The emission or absorption of 21-cm radiation from a neutral IGM is governed by the spin temperature T_S of the hydrogen, defined by

$$\frac{n_1}{n_0} = 3 \exp[-T_*/T_S], \quad (1)$$

where n_0 and n_1 are the singlet and triplet $n = 1$ hyperfine levels, $T_* \equiv h\nu_{10}/k_B = 0.07$ K, where ν_{10} is the frequency of the 21-cm transition, h is Planck's constant, and k_B is Boltzmann's constant. In the presence of only the Cosmic Microwave Background (CMB) radiation, the spin temperature will be the same as the temperature of the CMB, and no emission or absorption relative to the CMB will be detectable. A mechanism is required that decouples the two temperatures. This may be achieved by coupling the spin temperature to the kinetic temperature of the gas itself. Two mechanisms are available, collisions between hydrogen atoms (Purcell & Field 1956) and scattering by Ly α photons (Wouthuysen 1952; Field 1958). The collision-induced coupling between the spin and kinetic temperatures is dominated by the spin-exchange process between the colliding hydrogen atoms. The rate, however, is too small for realistic IGM densities at the redshifts of interest, although collisions may be important in dense regions, $\delta\rho/\rho \gtrsim 30[(1+z)/10]^{-2}$ (Madau, Meiksin, & Rees 1997).

Instead the dominant mechanism is likely to be Ly α scattering through the Wouthuysen-Field effect. This process mixes the hyperfine levels of neutral hydrogen in its ground state via an intermediate transition to the $2p$ state. An atom initially in the $n = 1$ singlet state may absorb a Ly α photon that puts it in an $n = 2$ state, allowing it to return to the triplet $n = 1$ state by a spontaneous decay. At this point, the astute student of quantum mechanics will ask how is it possible for electric dipole radiation (Ly α photons) to induce a spin transition? The key is spin-orbit coupling: it's the total angular momentum $F = I + J$ that counts. (Here I is the proton spin and J is the total electron angular momentum, $J = S + L$.) There are four hyperfine states involved, the $n = 1$ singlet ${}_0S_{1/2}$ and triplet ${}_1S_{1/2}$ states (the notation is ${}_FL_J$), and the two

triplet $n = 2$ states $1P_{1/2}$ and $1P_{3/2}$. The selection rule $\Delta F = 0, 1$ permits the transitions $0S_{1/2} \rightarrow 1P_{1/2}$, $1P_{3/2}$ and $1P_{1/2}$, $1P_{3/2} \rightarrow 1S_{1/2}$, and so effectively $0S_{1/2} \rightarrow 1S_{1/2}$ occurs via one of the $n = 2$ states.

When the IGM is highly opaque to the scattering of Ly α photons, as it is when still neutral, the large number of scatterings of Ly α photons in an ambient radiation field will ensure a Boltzmann distribution for the photon energies near the Ly α frequency, with a temperature given by the kinetic temperature T_K of the IGM (Field 1959). In this case, the spin temperature of the neutral hydrogen becomes¹

$$T_S = \frac{T_{\text{CMB}} + y_\alpha T_K}{1 + y_\alpha}, \quad (2)$$

where $T_{\text{CMB}} = 2.73(1 + z)$ K is the temperature of the CMB (Mather *et al.* 1994), and

$$y_\alpha \equiv \frac{P_{10}}{A_{10}} \frac{T_*}{T_K} \quad (3)$$

is the Ly α pumping efficiency. Here, $A_{10} = 2.9 \times 10^{-15} \text{ s}^{-1}$ is the spontaneous decay rate of the hyperfine transition of atomic hydrogen, P_{10} is the indirect de-excitation rate of the triplet via absorption of a Ly α photon to the $n = 2$ level, and $T_S \gg T_*$ was assumed. In the absence of Ly α pumping the spin temperature goes to equilibrium with the 21-cm background radiation field on a timescale $T_*/(T_{\text{CMB}}A_{10}) \approx 5 \times 10^4 \text{ yr}$, and neutral intergalactic hydrogen will produce neither an absorption nor emission signature. If y_α is large, $T_S \rightarrow T_K$, signifying equilibrium with the matter. A consideration of the net transition rates between the various hyperfine $n = 1$ and $n = 2$ levels above shows that the $1 \rightarrow 0$ transition rate via Ly α scattering is related to the total rate P_α by $P_{10} = 4P_\alpha/27$ (Field 1958). This relation and equation (2) are derived in the Appendix. In the limit $T_K \gg T_{\text{CMB}}$, the fractional deviation in a steady state of the spin temperature from the temperature of the CMB is

$$\frac{T_S - T_{\text{CMB}}}{T_S} \approx \left[1 + \frac{T_{\text{CMB}}}{y_\alpha T_K} \right]^{-1}. \quad (4)$$

There exists then a critical value of P_α which, if greatly exceeded, would drive $T_S \rightarrow T_K$. This thermalization rate is (Madau *et al.* 1997)

$$P_{\text{th}} \equiv \frac{27A_{10}T_{\text{CMB}}}{4T_*} \approx (5.3 \times 10^{-12} \text{ s}^{-1}) \left(\frac{1+z}{7} \right). \quad (5)$$

2.2. 21-cm Emission Efficiency

To illustrate the basic principle of the proposed observations, consider a region of neutral material with spin temperature $T_S \neq T_{\text{CMB}}$, having angular size on the sky which is large compared to a beamwidth, and radial velocity extent due

¹In the presence of a radio source, the antenna temperature of the radio emission should be added to T_{CMB} in equation 2. The radio emission may make an important contribution in the vicinity of a radio-loud quasar (Bahcall & Ekers 1969), and would itself permit the IGM to be detected in 21-cm radiation.

to the Hubble expansion which is larger than the bandwidth. Its intergalactic optical depth at $21(1+z)$ cm along the line of sight,

$$\tau(z) = \frac{3c^3 h^3 n_{\text{HI}}(0) A_{10}}{32\pi H_0 k_{\text{B}}^3 T_*^2 T_S} (1+z)^{1.5} \approx 10^{-2.9} h_{50}^{-1} \left(\frac{T_{\text{CMB}}}{T_S} \right) \left(\frac{\Omega_{\text{IGM}} h_{50}^2}{0.05} \right) (1+z)^{1/2}, \quad (6)$$

will typically be much less than unity. The experiment envisaged consists of two measurements, separated in either angle or frequency, such that one measurement, the fiducial, detects no line feature, either because there is no H I or because $T_S \approx T_{\text{CMB}}$, and the second at $T_S \neq T_{\text{CMB}}$. Since the brightness temperature through the IGM is $T_b = T_{\text{CMB}} e^{-\tau} + T_S (1 - e^{-\tau})$, the differential antenna temperature observed at the Earth between this region and the CMB will be

$$\delta T = (1+z)^{-1} (T_S - T_{\text{CMB}}) (1 - e^{-\tau}) \approx (0.011 \text{ K}) h_{50}^{-1} \left(\frac{\Omega_{\text{IGM}} h_{50}^2}{0.05} \right) \left(\frac{1+z}{9} \right)^{1/2} \eta, \quad (7)$$

where the 21-cm radiation efficiency is defined as

$$\eta \equiv x_{\text{HI}} \left(\frac{T_S - T_{\text{CMB}}}{T_S} \right). \quad (8)$$

Here x_{HI} refers to the neutral fraction of the hydrogen in the region for which $T_S \neq T_{\text{CMB}}$. As long as T_S is much larger than T_{CMB} (hence if there has been significant preheating of the intergalactic gas), $\eta \rightarrow x_{\text{HI}}$, and the IGM can be observed in emission at a level which is independent of the exact value of T_S . By contrast, when $T_{\text{CMB}} \gg T_S$ (negligible preheating), the differential antenna temperature appears, in absorption, a factor $\sim T_{\text{CMB}}/T_S$ larger than in emission, and it becomes relatively easier to detect intergalactic neutral hydrogen (Scott & Rees 1990).

2.3. Preheating the IGM

The role of the spin temperature is manifest in eq. (8): when $T_S < T_{\text{CMB}}$ the IGM absorbs 21-cm radiation from the CMB, while for $T_S > T_{\text{CMB}}$ the IGM emits 21-cm radiation in excess of the CMB. In the absence of decoupling mechanisms, $T_S = T_{\text{CMB}}$. The presence of Ly α photons with sufficient intensity will thus enable the IGM to be “seen.” The adiabatic expansion of the Universe will generally bring the kinetic temperature of the IGM well below the temperature of the CMB. Coupling T_S to T_K will permit the IGM to be detectable in absorption. If there are sources of radiation that heat the IGM, however, it may be possible instead to detect the IGM in emission.

Possible heating sources are soft x-rays from an early generation of QSOs or thermal bremsstrahlung emission produced by the ionized gas in the collapsed halos of young galaxies. In CDM-dominated cosmologies, the latter may be in sufficient number to heat the IGM above the CMB temperature by $z \approx 7$ (Madau *et al.* 1997).

While photons just shortward of the photoelectric edge are absorbed at the ionization front generated by a QSO source, photons of much shorter wavelength will be able to propagate to much greater distances. Most of the photoelectric

heating of the IGM by a QSO is accomplished by soft x-rays. The time required for the radiation at the light front to heat the intergalactic gas to a temperature above that of the CMB is typically 10% of the Hubble time. The H II region produced by a QSO will therefore be preceded by a warming front. Note that, as the X-ray-heated bubbles around QSOs will survive as fossils even after the quasar has died, several generations N_g of quasars may actually be responsible for preheating the entire IGM. For a typical QSO age of $t_Q \approx 3 \times 10^8 N_g^{-1/3}$ yr, the required QSO comoving space density to heat the entire IGM to a temperature above that of the CMB by $z \approx 6$ is $\sim 10^{-10} \text{ Mpc}^{-3} N_g^{-1}$. By comparison, the comoving space density of bright QSOs at $z = 4$ is $\sim 100 N_g$ times larger (Warren, Hewett, & Osmer 1994). If all bright galaxies undergo a quasar phase, QSOs must have a very short lifetime, and $N_g \sim 100$. Soft X-rays from a few bright QSO sources could then prevent collapsing structures, such as protoclusters while still in the linear regime, from being detected in 21-cm absorption against the CMB.

An additional heating source is the Ly α photon scattering itself. The average relative change in a Ly α photon's energy E after having been scattered by a hydrogen atom at rest is

$$\left\langle \frac{\Delta E}{E} \right\rangle = -\frac{h\nu_\alpha}{m_H c^2} \approx -10^{-8}, \quad (9)$$

where m_H is the mass of the hydrogen atom. (It should be noted that this is an approximation valid only for $h\nu_\alpha \gg kT_K$. In the opposite limit, energy will flow from the atoms to the photons.) Through recoil, energy is transferred from photons to atoms at a rate

$$\dot{E}_\alpha = -\left\langle \frac{\Delta E}{E} \right\rangle h\nu_\alpha P_\alpha. \quad (10)$$

where P_α is the Ly α scattering rate per H atom. In the case of excitation at the thermalization rate P_{th} , equation (10) becomes

$$\dot{E}_{\text{th}} = \frac{27}{4} \frac{(h\nu_\alpha)^2}{m_H c^2} \frac{A_{10} T_{\text{CMB}}}{T_*} \approx (220 \text{ K Gyr}^{-1}) \left(\frac{1+z}{7} \right), \quad (11)$$

(Madau *et al.* 1997). The characteristic timescale for heating the medium above the CMB temperature via Ly α resonant scattering at this rate is

$$\Delta t_{\text{heat}} = \frac{2}{9} \frac{m_H c^2 \nu_{10}}{h\nu_\alpha^2} A_{10}^{-1} \approx 10^8 \text{ yr}, \quad (12)$$

about 20% of the Hubble time at $z \approx 8$. The result is a finite interval of time during which Ly α photons couple the spin temperature to the kinetic temperature of the IGM before heating the IGM above the CMB temperature. If Ly α sources turned on at redshifts $z_\alpha \lesssim 10$, this interval would present a window in redshift space near $z \approx 8$ that would enable a large fraction of intergalactic gas to be observable at $\sim 160 \text{ MHz}$ in *absorption* against the CMB, and so isolate the epoch of First Light.

3. Scenarios

The calculations in this section were done in collaboration with Paolo Tozzi and Piero Madau.

Two cosmological models are considered, a tilted Cold Dark Matter model (tCDM) with $\Omega_0 = 1$, $H_0 = 50 \text{ kms}^{-1} \text{ Mpc}^{-1}$, and $\sigma_8 = 0.55$, designed to match both CMB measurements on large scales and the constraint on amplitude imposed by galaxy cluster abundances on small, and a flat open CDM model (OCDM) with $\Omega_0 = 0.3$, $\Omega_\Lambda = 0.7$, $H_0 = 70 \text{ kms}^{-1} \text{ Mpc}^{-1}$, and $\sigma_8 = 1.1$, which similarly matches both constraints. The baryon density in both models is assumed to be $\Omega_B h^2 = 0.024$, where $h = H_0/100 \text{ kms}^{-1} \text{ Mpc}^{-1}$.

We consider a scenario in which sources of Ly α photons are in sufficient abundance throughout the universe to couple the spin temperature to the kinetic temperature of the IGM everywhere. We further suppose the IGM has been preheated to a temperature well above that of the CMB, either by the same Ly α photons responsible for the coupling or by soft x-ray sources. In this case, the IGM will emit at a rate independent of T_S (the hyperfine levels will be occupied according to their statistical weights, $n_1/n_0 = 3$). Because of structure in the IGM, the emission will not be uniform.

In Figure 1, we show the range of density fluctuations that would be detectable in a single beam by a Square Kilometre Array Interferometer (SKAI) at 160 MHz ($z = 8$), as a function of beam size and frequency band width, and for several assumed integration times. The detection thresholds are scaled according to a continuum *rms* in a 80 MHz band at 160 MHz of 64 nJy over an 8 hour integration time (Braun 1998; also see www.nfra.nl/skai/science/index.htm). The experiment is based on taking differences between beams. The dashed lines show curves of constant *rms* antenna temperature fluctuation within the IGM, $\langle (\delta T_a)^2 \rangle^{1/2} = \sigma_\rho \bar{T}_a$, where σ_ρ is the *rms* relative density fluctuation of the IGM for a volume corresponding to a given bandwidth ($\Delta\nu/\nu = \Delta z/[1+z]$) and angular size $\Delta\theta$. Here, \bar{T}_a is the mean antenna temperature from the IGM at redshifted 21-cm. At a fixed bandwidth, the antenna temperature fluctuation increases with decreasing angular scale because σ_ρ increases with decreasing linear scale. Because the detected flux is proportional to the solid angle of the beam, the detected signal decreases with decreasing angular scale until it falls below the detection threshold, indicated by the solid lines. The size of the detectable IGM fluctuations differs greatly for the two models. This is because the growth of density fluctuations ceases early on in an open universe, so that the fluctuations on a given angular scale are much larger in the OCDM model than in tCDM at high redshift.

In a second scenario, the spin temperature is again coupled to the IGM kinetic temperature everywhere, but the IGM has not had time to heat above the CMB temperature. We then consider the emission signature resulting from a QSO soon after it turns on as the medium surrounding it is heated by soft x-rays from the QSO. The experiment in this case is done by differencing beams pointed in regions around the QSO with one pointed through the QSO H II region, where both emission and absorption are absent. An image of the resulting emission for the tCDM model is shown in Figure 2. The model was computed using Hydra (Couchman, Thomas, & Pearce 1995). As the warming front produced by the QSO expands, a growing amount of the surrounding IGM is revealed. Note that,

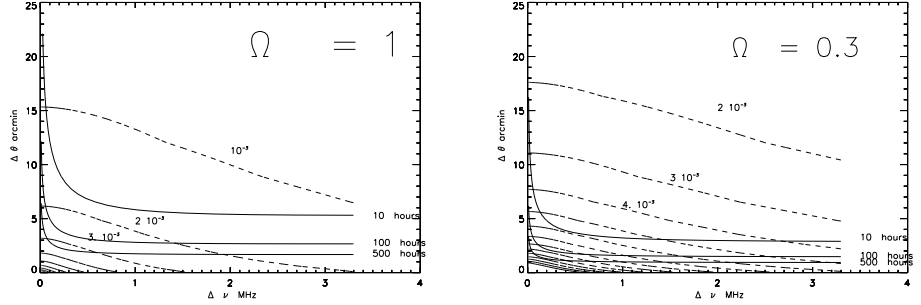


Figure 1. Detectability of fluctuations in 21-cm brightness temperature ($10^{-3} < \langle (\delta T_a)^2 \rangle^{1/2} < 10^{-2}$), from the IGM by SKAI as a function of beam width and bandwidth. The dashed lines show the size of the *rms* fluctuations expected in a volume defined by the angle and frequency widths. The solid lines show the threshold below which the fluctuations are undetectable for integration times of 10, 100, and 500 hours.

although the QSO was placed in the corner of the simulation volume, the figure can equally be viewed as the emission due to heating by a beam of soft x-rays from the QSO with an opening angle of 90° . Thus imaging the gas surrounding a QSO in 21-cm emission would provide a direct means of measuring the opening angle of QSO emission.

It should also be noted that a region of a given fixed density fluctuation will not always yield the same fluctuation in 21-cm emission. This is because of the dependence of the spin temperature on the temperature of the IGM. Only when the IGM temperature much exceeds that of the CMB will the 21-cm emission be independent of the IGM temperature, according to equation (8). In general, the fluctuations in brightness temperature will depend on both the density fluctuations of the IGM and the temperature fluctuations, which in turn depend on the ages and distribution of the sources. A knowledge of the cosmological density fluctuation spectrum, as may be measured by future CMB missions like MAP and Planck, will then enable the statistical distribution of the sources that heat the IGM, whether QSOs as here or $\text{Ly}\alpha$ photons from early stars, to be established using measurements of the fluctuations in the 21-cm sky at high redshift.

Acknowledgments. I thank P. Madau and R. Taylor for financial support to attend the SKA Workshop.

References

- Bahcall, J. N., & Ekers, R. D. 1969, ApJ, 157, 1055
- Braun, R., ed., 1998, SKART Science Case
- Couchman, H. M. P., Thomas, P. A., & Pearce, F. R. 1995, ApJ, 452, 797
- Dey, A., Spinrad, H., Stern, D., Graham, J. R., & Chaffee, F. H. 1998, ApJ, 498, L93

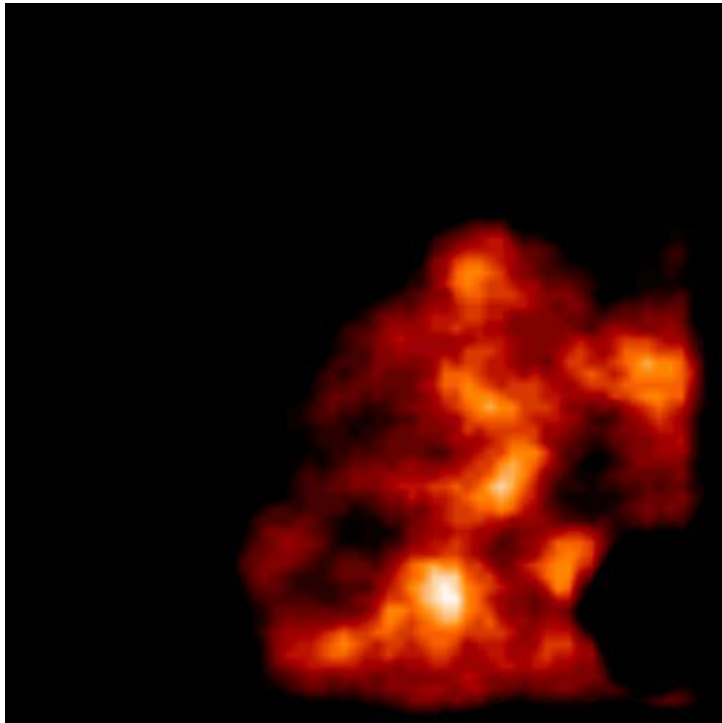


Figure 2. 21-cm emission from the region surrounding a QSO source (lower right) revealed once the region is heated above the temperature of the Cosmic Microwave Background by soft x-rays from the QSO.

- Field, G. B. 1958, Proc. I.R.E., 46, 240
 ———. 1959, ApJ, 129, 551
 Governato, F., Gardner, J. P., Stadel, J., Quinn, T., & Lake, G. 1997, preprint, astro-ph/9710140
 Haardt, F. & Madau, P. 1996, ApJ, 461, 20
 Hughes, D., *et al.* 1998, preprint, astro-ph/9806297
 Madau, P., Meiksin, A., & Rees, M. J. 1997, ApJ, 475, 429
 Madau, P., Pozzetti, P., & Dickinson, M. 1998, ApJ, 498, 106
 Mather, J. C., *et al.* 1994, ApJ, 420, 439
 Meiksin, A., & Madau, P. 1993, ApJ, 412, 34
 Purcell, E. M., & Field, G. B. 1956, ApJ, 124, 542
 Scott, D., & Rees, M. J. 1990, MNRAS, 247, 510
 Warren, S. J., Hewett, P. C., & Osmer, P. S. 1994, ApJ, 421, 412
 Wouthuysen, S. A. 1952, AJ, 57, 31
 Zhang, Y., Meiksin, A., Anninos, P., & Norman, M. L. 1998, ApJ, 495, 63

A The Wouthuysen-Field Mechanism

There are six hyperfine states in total that contribute to the Ly α transition. These are shown in Figure 3. Only four of these, the two $n = 1$ states and the two $n = 2$, $F = 1$ states, contribute to the excitation of the 21-cm line by Ly α scattering. Denoting the occupation number of $_0S_{1/2}$ by n_0 and that of $_1S_{1/2}$ by n_1 , the rate equation for n_0 is

$$\frac{dn_0}{dt} = A_{10} \left(1 + \frac{T_R}{T_*} \right) n_1 - 3A_{10} \frac{T_R}{T_*} n_0 + P_{10}^\alpha n_1 - P_{01}^\alpha n_0, \quad (13)$$

where the radiation intensity at the 21-cm frequency has been expressed in terms of the antenna temperature T_R , $I_{10} = 2k_B T_R / \lambda_{10}^2$. The ratio T_R/T_* is the number of 21-cm photons per mode. Here, P_{01}^α and P_{10}^α are the effective excitation and de-excitation rates due to Ly α scattering. These may be related to the total scattering rate of Ly α photons, P_α , as is now shown.

It is convenient to label the $n = 2$ levels as states 2–5, from lowest energy to highest. Then the external radiation intensity at the frequency ν_{ij} corresponding to the $i \rightarrow j$ transition may be expressed as the antenna temperature T_R^{ij} , as above. The temperature corresponding to the energy difference itself, $h\nu_{ij}$, is expressed as $T_{ij} = h\nu_{ij}/k_B$. If A_{ji} denotes the spontaneous decay rate for the transition $j \rightarrow i$, then P_{01}^α and P_{10}^α are given by

$$P_{01}^\alpha = 3 \frac{T_{03}^R}{T_{03}} \frac{A_{30}A_{31}}{A_{30} + A_{31}} + 3 \frac{T_{04}^R}{T_{04}} \frac{A_{40}A_{41}}{A_{40} + A_{41}} \quad (14)$$

and

$$P_{10}^\alpha = \frac{T_{13}^R}{T_{13}} \frac{A_{30}A_{31}}{A_{30} + A_{31}} + \frac{T_{14}^R}{T_{14}} \frac{A_{40}A_{41}}{A_{40} + A_{41}}. \quad (15)$$

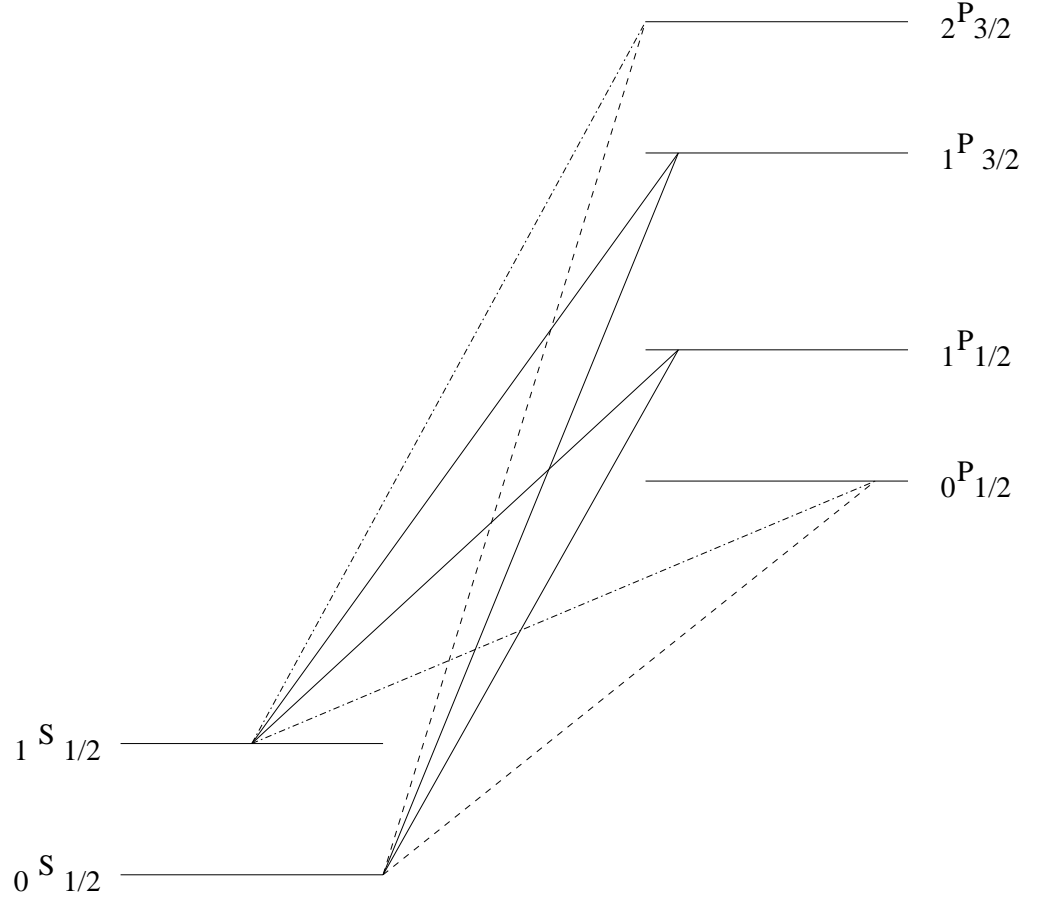


Figure 3. The hyperfine energy level diagram for the Ly α transition. The two $n = 1$ states are on the left, and the $n = 2$ states are on the right. The dashed lines represent forbidden transitions ($F = 0 \rightarrow F = 0$ and $\Delta F = 2$ are not permitted), while the dot-dashed lines represent complementary transitions that give no contribution to the excitation or de-excitation of the 21-cm transition.

The ratios A_{ji}/A_α , where A_α is the total Ly α spontaneous decay rate, may be solved for using a sum rule for the transitions. This states that the sum of all transitions of given nFJ to all the $n'J'$ levels (summed over F' and $m_{F'}$) for a given $n'J'$ is proportional to $2F+1$.² There are four sets of downward transitions to $n' = 1$, $J' = 1/2$, corresponding to the decay intensities I_{51} , $I_{50}(= 0)$, I_{41} , I_{40} , I_{31} , I_{30} , I_{21} , and $I_{20}(= 0)$. These give

$$\frac{I_{51}}{I_{40} + I_{41}} = \frac{5}{3}, \quad \frac{I_{40} + I_{41}}{I_{30} + I_{31}} = 1, \quad \frac{I_{30} + I_{31}}{I_{21}} = 3. \quad (16)$$

Similarly, there are four sets of upward transitions to $n' = 2$, $J' = 1/2$ or $3/2$, giving the intensities I_{30} , $I_{20}(= 0)$, I_{31} , I_{21} , $I_{50}(= 0)$, I_{40} , I_{51} , and I_{41} . These ratios are

$$\frac{I_{40}}{I_{41} + I_{51}} = \frac{1}{3}, \quad \frac{I_{30}}{I_{21} + I_{31}} = \frac{1}{3}. \quad (17)$$

Using $I_{kj}/I_\alpha = (g_k/g_{\text{tot}})(A_{kj}/A_\alpha)$, where I_α is the total Ly α decay intensity summed over all the hyperfine transitions, and $g_k = 2F + 1$ is the statistical weight of level k (g_{tot} is the sum of the weights of the upper levels), gives $A_{20}/A_\alpha = A_{50}/A_\alpha = 0$, $A_{21}/A_\alpha = A_{51}/A_\alpha = 1$, $A_{30}/A_\alpha = A_{41}/A_\alpha = 1/3$, and $A_{31}/A_\alpha = A_{40}/A_\alpha = 2/3$. We then obtain $P_\alpha = 3A_\alpha(T_R/T_\alpha)$ ($T_\alpha \equiv h\nu_\alpha/k_B$), and $P_{10} = (4/27)P_\alpha$. Statistical equilibrium for $T_R = 0$ requires $P_{01}/P_{10} = n_1/n_0 = 3 \exp(-T_*/T_K)$. Solving the rate equation (13) for $T_R > 0$ gives equation (2), where $T_R = T_{\text{CMB}}$, and where $T_S \gg T_*$, $T_K \gg T_*$, and $T_R \gg T_*$ have been assumed.

²See, e.g., Bethe, H. A., Salpeter, E. E. 1957, *Quantum Mechanics of One- and Two-Electron Atoms*, New York: Academic Press.